X-ray Crystal Structure and Luminescence Properties of Pd(II) and Pt(II) Complexes with Dithiopyrrole

Jun-Gill Kang,[*] **Dong-Hee Cho, Changmoon Park, Sung Kwon Kang, In Tae Kim,**[†,*] **Sang Woo Lee,**[†]
Ha Hyeong Lee,[†] **Young Nam Lee,**[†] **Dae Won Lim,**[†] **Sung Jae Lee,**[†] **Sung Ho Kim,**[†] **and Young Ju Bae**[†]

Department of Chemistry, Chungnam National University, Daejeon 305-764, Korea. [*]*E-mail: jgkang@cnu.ac.kr*
[†]*Department of Chemistry, Kwangwoon University, Seoul 139-701, Korea.* [*]*E-mail: itkim@kw.ac.kr*
Received November 1, 2007

The complexes Pd(nbmtp)Cl$_2$ and Pt(nbmtp)Cl$_2$ (nbmptp = 1-nonyl-3,4-bis(methylthio)pyrrole) were prepared and their x-ray structures were determined at room temperature. The four-coordinated metal unit and the pyrrole ring formed a nearly planar geometry. The free ligand dissolved in CH$_2$Cl$_2$ produced two luminescence bands associated with the lone-pair electron of S (λ_{max} = 525 nm) and the pyrrole π electron (λ_{max} = 388 nm). When the two complexes were dissolved in CH$_2$Cl$_2$, these two luminescence bands were also observed, although the low-energy band was blueshifted. For the crystalline Pt(II) complex, only the strong charge transfer band (λ_{max} = 618 nm) from the d^* orbital of Pt resulted from excitation of the lone-pair electron of S.

Key Words : Pt(II) bis(methylthio)pyrrole, Pd(II) bis(methylthio)pyrrole, X-ray structure, Luminescence
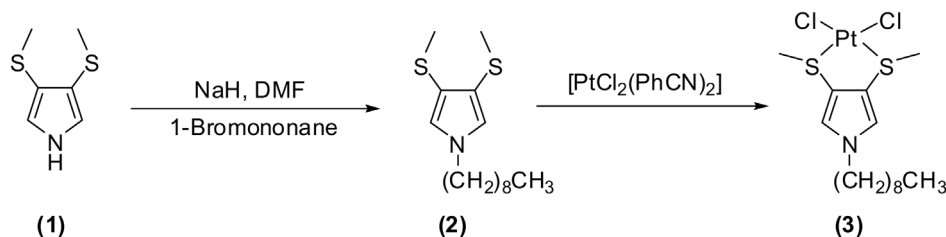
Introduction

The electronic structure and transitions of square-planar complexes of platinum(II) and palladium(II) with d^8 electronic configuration have been investigated extensively for various ligand systems, such as halide, N-donor ligands, and S-donor ligands.[1-6] The luminescence of these complexes is very weak at room temperature because of the spin-forbidden $d \rightarrow d$ transition and the presence of low-energy ligand-field excited states, causing a nonradiative transition. For the thiocyanate and selenocyanate complexes, the application of external pressure induces luminescence by destabilizing the lowest unoccupied molecular orbital.[7-9] Some planar mononuclear Pd(II) and Pt(II) complexes, however, are emissive at ambient temperature and pressure. The luminescence of these complexes has been interpreted in terms of a inter-ligand charge-transfer (ILCT),[10,11] metal-to-ligand charge transfer (MLCT),[12,13] or a mixed of both.[14,15] Previously, we prepared the titled Pd(II) complex and characterized its crystal structure and luminescence property.[16] The complex dissolved in CH$_2$Cl$_2$ produced luminescence in the 325-650 nm region. This study investigated the single-crystal x-ray structure and optical properties of dichloro1-nonyl-3,4-bis(methylthio)pyrrole platinum(II), [Pt(nbmtp)Cl$_2$]. The optical properties of the free ligand and the Pd(II) complex were also studied to reveal the absorbing and emitting levels

of planar M(II) complexes. This work is important for delineating the luminescent properties of related mononuclear Pd(II) and Pt(II) complexes, for which the optical processes and their relationship to different structural conformations are debated.

Experimentals

Synthesis and crystal growth. Previously, we reported the syntheses of nbmptp and its Pd(II) complex.[16] Similarly, we prepared Pt(nbmtp)Cl$_2$, as shown in Scheme 1. The nbmpt ligand (0.15 g, 1.1 mmol)(**2**) was added to a solution of [PtCl$_2$(PhCN)$_2$] (0.25 g, 1.1 mmol) in dry chloroform (20 mL). After stirring at 35 °C for 11 h, the chloroform was evaporated and the resulting yellow powder was purified by column chromatography on silica gel (dichloromethane: hexane = 3:7) to afford 0.24 g (82%) of **3** as a yellow powder. Single crystals were grown in the hexane and benzene solution by using a slow evaporation method. ^{1}H NMR (400 MHz, CDCl$_3$) δ 7.03-6.99 (d, 2H), 3.97-3.91 (q, 2H), 2.94-2.87 (d, 6H), 1.83-1.81 (m, 2H), 1.30-1.25 (m, 12H), 0.89-0.85 (t, 3H); ^{13}C NMR (100 MHz, CDCl$_3$) δ 121.8, 120.4, 52.4, 31.7, 31.5, 30.9, 29.2, 29.0, 28.9, 26.4, 22.5, 14.0. Anal. Calcd for C$_{15}$H$_{27}$Cl$_2$PtNS$_2$: C, 32.67; H, 4.93; N, 2.54; S, 11.63. Found: C, 32.82; H, 4.95; N, 2.57; S, 11.81.
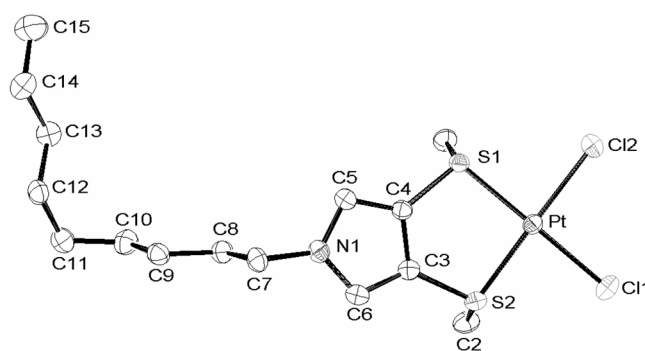
Determination and refinement of the X-ray Structure.

Scheme 1

Table 1. Crystallographic Data and Refinement Details for Me(nbmtp)Cl$_2$ (Me = Pd and Pt)

Compound	Pd	Pt
Formula	C$_{15}$H$_{27}$Cl$_2$PdNS$_2$	C$_{15}$H$_{27}$Cl$_2$PtNS$_2$
Formula weight	462.80	551.49
Crystal system	monoclinic	monoclinic
Space group	$P2_1/C$	$P2_1/C$
a (Å)	7.7838(8)	7.72880(10)
b (Å)	16.3784(13)	16.3515(3)
c (Å)	15.5354(10)	15.3482(3)
β (°)	90.136(8)	90.4760(10)
V (Å^3)	1980.5(3)	1939.60(6)
Z	4	4
D_{cal} (mg m^{-3})	1.552	1.889
$F(000)$	944	1072
μ (mm^{-1})	1.412	7.719
θ rang (°)	1.81-28.31	1.82-28.30
Reflections collected /unique [R(int)]	40392/4927 [0.0717]	20684/4817 [0.0296]
Completeness (%) [to θ(°)]	99.9 [28.31]	99.9 [28.30]
Data/restraints/parameters	4927/0/190	4817/0/192
Goodness-of-fit on F^2	1.010	1.036
R1, ωR2 with $I \geq 2.0\sigma(I)$		
final	0.0377, 0.0708	0.0176, 0.0397
All data	0.0816, 0.0842	0.0213, 0.0407
Largest diff. peak	0.401	0.939
hole (e Å^{-3})	−0.581	−0.500

Intensity data were collected at room temperature on a Bruker P4 diffractometer fitted with Mo-Kα radiation. The intensities were corrected for Lorentz-polarization effects, and empirical absorption correction (Ψ scan) was also applied. The structures of the titled compounds were solved by applying the direct method using SHELXTL[17a] and refined by a full-matrix least-squares refinement on F using SHELEX97.[17b] Typically, the refinement was on F^2, applying data that had been corrected for absorption effects using an empirical procedure, with non-hydrogen atoms modeled with anisotropic displacement parameters and hydrogen atoms in their calculated positions, and using a weighting scheme of the form $w = 1/[^2(F_o^2) + (aP)^2 + bP]$ where $P = (F_o^2 + 2F_c^2)/3$. The crystal data and refinement results are summarized in Table 1.

Optical measurements. The UV-vis spectra of the free ligand and the two complexes were recorded at room temperature on a Shimadzu UV-2401PC spectrophotometer with a 1-cm path-length quartz cell. All samples were dissolved in CH$_2$Cl$_2$ for spectroscopic measurement, and the concentrations were adjusted to approximately 10^{-3}-10^{-4} M. To measure luminescence and excitation spectra, samples in microcrystalline state were placed on the cold finger of a CTI-cryogenics refrigerator using silicon grease. Excited light from an Oriel 1000-W Xe arc lamp was passed through an Oriel MS257 monochromator and focused on the sample. The spectra were measured at a 90° angle with an ARC 0.5 m Czerny-Turner monochromator equipped with a cooled

Figure 1. Perspective ORTEP drawing of the Pt(II) complex, showing the atom-numbering. Thermal ellipsoids of 50% are shown.
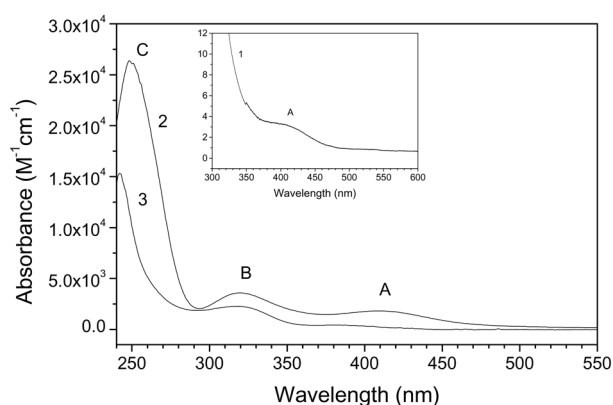
Hamamatsu R-933-14 photomultiplier tube. Photoluminescence (PL) spectra were measured with a He-Cd 325-nm laser line.

Results and Discussion

Crystal structures. The complex crystallizes in the monoclinic space P2$_1$/c. Figure 1 shows a perspective view of the crystalline form for the Pt(II) complex, in which the Pt(II) ion forms a four-coordinated complex with two Cl and two S atoms. Some selected geometric parameters for the Pt(II) complex are compared with those of the Pd(II) complex in Table 2. The crystal contained a discrete mononuclear unit of the complex, As listed in Table 2, the Pt-S distances were 2.2660(6) and 2.2555(6) Å, which were slightly shorter than those of the Pd(II) complex (2.2795(9) and 2.2763(10) Å). The Pt-Cl distances of 2.3174(6) and 2.3194(6) Å were slightly longer than those of Pd-Cl (2.3051(10) and 2.3099(10) Å). The sum of angles about the

Table 2. Selected bond lengths (Å) and bond angles (°) of Pd(nbmtp)Cl$_2$ (2) and Pt(nbmtp)Cl$_2$

	Pd	Pt
Me-S(1)	2.2795(9)	2.2660(6)
Me-S(2)	2.2763(10)	2.2555(6)
Me-Cl(1)	2.3051(10)	2.3174(6)
Me-Cl(2)	2.3099(10)	2.3194(6)
S(1)-C(1)	1.816(3)	1.812(2)
S(1)-C(4)	1.756(3)	1.757(2)
S(2)-C(2)	1.812(4)	1.813(3)
S(2)-C(3)	1.753(4)	1.754(2)
N(1)-C(5)	1.362(4)	1.365(3)
N(1)-C(6)	1.363(4)	1.361(3)
N(1)-C(7)	1.470(4)	1.471(3)
S(2)-Me-S(1)	92.27(3)	92.69(2)
S(2)-Me-Cl(1)	86.59(4)	86.81(2)
S(1)-Me-Cl(2)	87.21(4)	87.83(2)
Cl(1)-Me-Cl(2)	93.93(4)	92.67(2)
C(4)-S(1)-Me	101.52(12)	101.32(8)
C(3)-S(2)-Me	101.40(12)	101.81(8)
C(5)-N(1)-C(6)	110.0(3)	110.4(2)
C(5)-N(1)-C(7)	125.4(3)	124.9(2)
C(6)-N(1)-C(7)	124.6(3)	124.7(2)

Crystal Structure and Luminescence

Bull. Korean Chem. Soc. **2008**, Vol. 29, No. 3   601

Figure 2. Absorption spectra of nbmptp (1), Pd(nbmtp)Cl₂ (2) and Pt(nbmtp)Cl₂ (3) dissolved in CH₂Cl₂.

Figure 3. Luminescence and excitation spectra of nbmpt dissolved in CH₂Cl₂ (concentration: 1×10^{-4} M): (1) $\lambda_{exn} = 402$ nm and $\lambda_{ems} = 527$ nm, and (2) $\lambda_{exn} = 322$ nm and $\lambda_{ems} = 388$ nm.
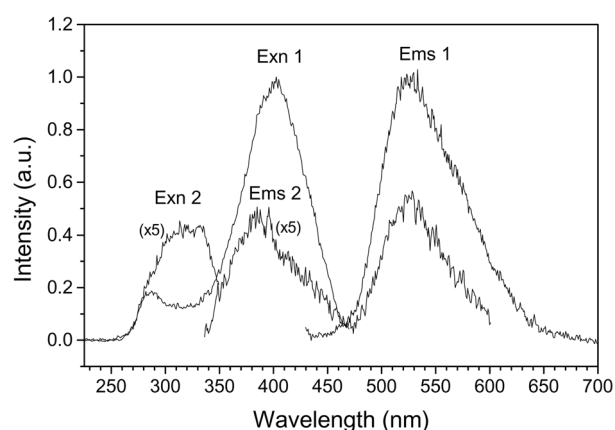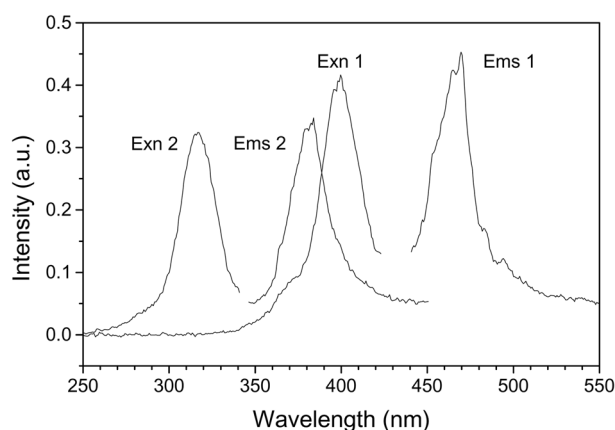
two metal ions was exactly 360.00°. The root mean square (rms) deviation of the five atoms from the least-square's plane was only 0.0003 Å for the Pd(II) complex and 0.0039 Å for the Pt(II) complex. These results indicate that the four-coordinated metal unit was almost square planar. The coordination of the metal ion to two S atoms resulted in a five-member ring between the metal ion and pyrrole ring. The rms deviation of the five atoms from the least-square's plane is 0.0320 Å for the Pd(II) complex and 0.0309 Å for the Pt(II) complex, indicating that the five-member ring was almost square planar. It should be noted that there is week π interaction between 5-membered ring and one of hydrogen atom on C11 atom. The bond distances between H atom and center of ring are 2.94 and 2.83 Å for Pd and Pt complexes, respectively.

Absorption, luminescence and excitation spectra. The absorption spectra of the free ligand, and the Pd(II) and Pt(II) complexes dissolved in CH₂Cl₂ are shown in Figure 2. The Pd(II) complex produced two weak absorption bands peaking at 409 nm and 320 nm and a strong band at 248 nm. Hereafter, these bands are referred to as A-, B- and C-absorption bands in order of increasing energy. The Pt(II) complex also produced three absorption bands: these three bands were slightly blue-shifted and appeared at 388, 319 nm and 238 nm, respectively. In contrast, for the free ligand, the A- and B-absorption bands were almost forbidden. The A-absorption band appeared as a trace only (see the spectrum inserted in Figure 2). The intensities of these two bands were enhanced considerably by the complexation with Pd(II) and Pt(II). The absorption data are summarized in Table 3.

The luminescence and excitation spectra of the free ligand and the complexes dissolved in CH₂Cl₂ were measured at room temperature. As shown in Figure 3, the free ligand

excited in UV light produced two luminescence bands, peaking at 527 and 388 nm. The low-energy 527 nm emission was produced by the 402 nm excitation, and weak emission was also produced by the 280 nm excitation. The 402 nm excitation and the 527 nm emission bands were mirror images. The high-energy 388 nm emission was weakly induced by the 322 nm excitation. The peak positions of these two excitation bands were almost coincided with the A- and the B-absorption bands of the complexes, respectively, which were forbidden for the free ligand. Accordingly, the low- and high-energy emissions were referred to as the A- and B-band emissions, respectively. Note that the Stokes shift Δ of the A-band emission (5900 cm⁻¹) almost equaled that of the B-band emission (5790 cm⁻¹). Previously, we reported the luminescence properties of pyrrole and thio derivatives. The luminescence properties of the low- and the high-energy bands were very similar to those of pyrrole[18] and thiol derivatives,[19] respectively. The pyrrole monomer and the thiol derivatives produced weak violet and green luminescence, respectively. The peak positions of the excitation spectra of the A- and B-band emissions were in good agreement with those of the thiol and pyrrole derivatives, respectively. The similar features led us to assign the A-band emission as the $\sigma^* \rightarrow n$ transition of the methylthio group and the B-band emission as the π^*

Table 3. Electronic absorption data (recorded in CH₂Cl₂ solution) for Pd(nbmtp)Cl₂ (2) and Pt(nbmtp)Cl₂

compound	λ/nm ($\varepsilon \times 10^{-3}$/M⁻¹ cm⁻¹)
Pd(II)	248(26.4), 320(2.7), 409(1.8)
Pt(II)	238(14.2), 319(1.2), 388(0.4)

Table 4. Excitation and emission data and assignment of emissive transitions for nbmtp, Pd(nbmtp)Cl₂ and Pt(nbmtp)Cl₂

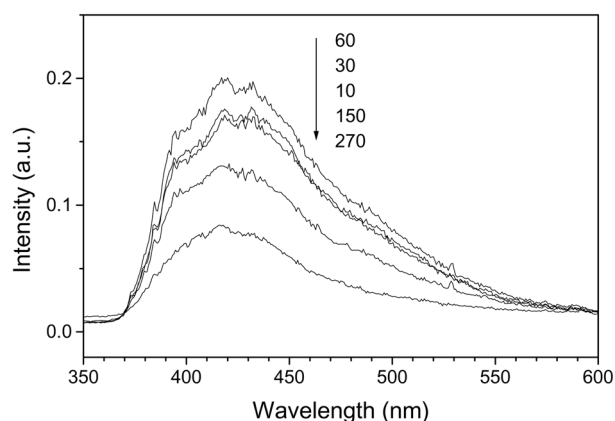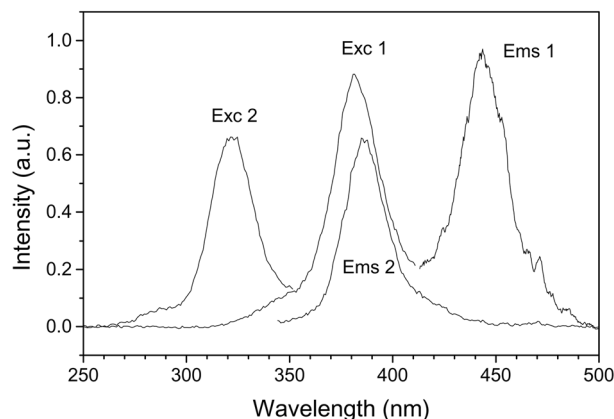| compound	excitation/nm	emission/nm	emissive transition
nbmtp	403	525	$\sigma^* \rightarrow n$ (S)
	320	388	$\pi^* \rightarrow \pi$ (pyrrole)
Pd(II)			
CH₂Cl₂	400	470	$\sigma^* \rightarrow n$ (S)
	319	384	$\sigma^* \rightarrow n$ (S)
Crystal		no emission	
Pt(II)			
CH₂Cl₂	382	444	$\sigma^* \rightarrow n$ (S)
	321	386	$\sigma^* \rightarrow n$ (S)
Crystal	420 - 450	618	MLCT: d (Pd) $\rightarrow n$ (S)

Figure 4. Luminescence and excitation spectra of Pd(nbmtp)Cl$_2$ dissolved in CH$_2$Cl$_2$ (concentration: 1×10^{-3} M): (1) $\lambda_{exn} = 400$ nm and $\lambda_{ems} = 470$ nm, and (2) $\lambda_{exn} = 317$ nm and $\lambda_{ems} = 382$ nm.

$\rightarrow \pi$ transition of the pyrrole ring. The excitation and emission data of the free ligand are summarized in Table 4.

Figure 4 shows the luminescence and excitation spectra of the Pd(II) complex dissolved in CH$_2$Cl$_2$. The A-band excitation produced a strong emission band peaking at 470 nm. Although the peak position of the A-band excitation of the Pd(II) complex is the same to that of the free ligand, the A-band emission was blue-shifted by about 2300 cm^{-1} compared to the case of the free ligand. Since the excitation and emission spectra were mirror images, we attributed the A-band emission to intra ligand transitions associated with the thiol group. The blueshift of the A-band emission indicated that the σ^* orbital of S became more destabilized due to the coordination of one lone-pair electron of S to Pd compared to the case of the free ligand. For the B-band, the peak positions of the emission and excitation bands of the Pd(II) complex are identical to those of the free ligand. As shown in Figure 4, the B-band excitation produced the 384 nm emission from the Pd(II) complex. The difference in the B-band emission between the free ligand and the complex was only the intensity. We also measured the luminescence spectrum of the Pd(II) complex in the crystalline state as a function of temperature. Unexpectedly, the A-band excita-
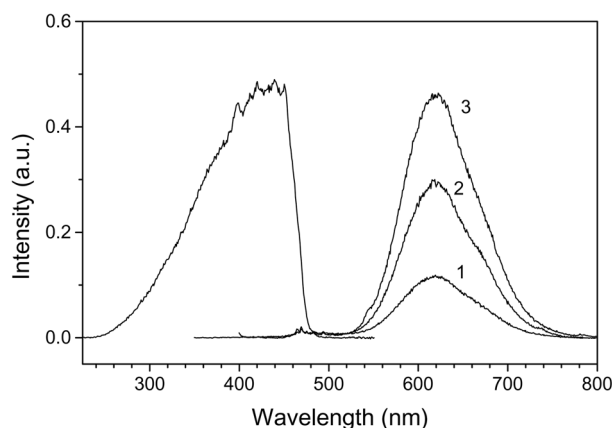

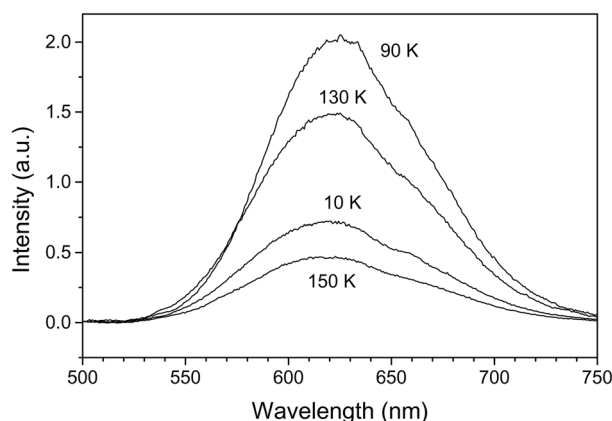**Figure 5**. PL spectra of Pd(nbmtp)Cl$_2$ crystals measured at various temperature ($\lambda_{exn} = 325$).

Figure 6. Luminescence and excitation spectra of Pt(nbmtp)Cl$_2$ dissolved in CH$_2$Cl$_2$ (concentration: 1×10^{-3} M): (1) $\lambda_{exn} = 382$ nm and $\lambda_{ems} = 402$ nm, and (2) $\lambda_{exn} = 323$ nm and $\lambda_{ems} = 386$ nm.

tion did not produce the emission from the Pd(II) complex in the crystalline state. As shown in Figure 5, at T = 10 K, the crystal excited by a He-Cd 325-nm line produced weak B-band emission, for which the peak position was red-shifted compared to the case for the solution state. With increasing temperature, the intensity increased and became maximal at 60 K. Above T = 60 K, the intensity decreased with increasing temperature.

As shown in Figure 6, the Pt(II) complex also exhibited spectral features similar to those of the Pd(II) complex. The A-band and B-band excitations produced the 442 and 387 nm emission bands, respectively. The B-band peak positions of the emission and excitation equaled to those of the free ligand. Although the peak position of the A-band excitation was almost equal to the case of the free ligand, the A-band emission was markedly blueshifted by about 3640 cm^{-1} compared to the case of the free ligand. In the case of the Pd(II) complex, the anti-bonding σ^* orbital of S was destabilized by the coordination to Pd(II). Similarly, the A-band and the B-band emissions were attributed to the intraligand transitions associated with the lone-pair electron of the sulfur atom and the π electron of the pyrrole ring, respectively. The Pt(II) complex in the crystalline state did not produce any luminescence at room temperature, while at T = 10 K, the crystals produced characteristic luminescence and excitation bands, as shown in Figure 7. Single crystals of the Pt(II) complex excited by UV produced a single emission band, peaking at 620 nm. Platinum dithiolate complex shows the similar emission feature, in which the 625 nm emission band was observed at 77 K.[20] As shown in Figure 8, with increasing temperature, the intensity increased and became maximal at T = 90 K. Above this temperature, the intensity decreased with increasing temperature and none was observed at room temperature. The excitation spectrum of the 620 nm emission was very broad, ranging from 300 to 480 nm. These spectral features of the crystalline state were significantly different from those of the solution state. These results led us to postulate that the 620 nm emission from the Pt(II) complex in the crystalline state was associated with the MLCT transition. The lone-pair electron of S was

Crystal Structure and Luminescence

Bull. Korean Chem. Soc. **2008**, Vol. 29, No. 3   603

Figure 7. Luminescence (λ_{exn} = 1; 317, 2; 381 and 3; 445 nm) and excitation (λ_{ems} = 618 nm) spectra of the Pt(II) complex in crystalline state at T = 10 K.

Figure 8. Luminescence spectra of Pt(nbmtp)Cl$_2$ crystals measured at various temperature (λ_{exn} = 440).

strongly associated with the charge transfer transition since the excitation energy was slightly lower than the A-band excitation energy.

The quantum mechanical calculation was performed using SDD basis functions (LanL2DZ for Pt; 6-31G(d) for S and Cl; 6-31G for H, C, N and O).[21] The molecular-orbital calculation suggested that the lowest unoccupied orbital (LUMO) is the $d_{x^2-y^2}$ orbital of Pt, forming a σ^* orbital with S, by taking the molecular axis along the x-axis under the C$_{2v}$ symmetry. For [Pt(II)X$_4$]$^{2-}$, the $d_{x^2-y^2}$ orbital was found as the LUMO.[22] The next LUMOs were split p orbitals of Pt and the other d orbitals were much higher than these p orbitals. Accordingly, the LUMO $d_{x^2-y^2}$ orbital of Pt was associated with the 620 nm band of the Pt(II) complex in the crystalline state. The LUMO $d_{x^2-y^2}$ orbital of Pt was populated *via* n(S) $\rightarrow d_{x^2-y^2}$ (Pt) LMCT and consequently emitted the red luminescence *via* MLCT.

Conclusion

In the solution, the free ligand and its metal complexes excited by UV light produced two emission bands. The low-energy A-band and the high-energy B-band emissions were associated with the lone-pair electron of S and the π electron of the pyrrole, respectively. The A-band emission was markedly affected by coordinating to the metal: the coordination of one of the lone-pair electrons of S resulted in the blue-shift in the A-band emission. In the crystalline state, the Pt(II) complex produced the charge-transfer emission via the excitation of the lone-pair electron of S in main and the excitation of the π electron of the pyrrole in minor. Unexpectedly, the crystalline Pd(II) complex produced the B-band emission only, but its intensity was very weak, even at low temperatures.

Supplementary Materials. Supplementary data associated with this article can be obtained free of charge from the Cambridge Crystallographic Data Centre (CCDC 650333 for Pd(nbmtp)Cl$_2$ and CCDC 665254 for Pt(nbmtp)Cl$_2$).

References

1. Lever, A. B. P. *Inorganic Electronic Spectroscopy*, 2nd Ed.; Elsevier: Amsterdam, 1984; Chapter 6.
2. Vanquickenborne, L. G.; Ceulemans, A. *Inorg. Chem.* **1981**, *20*, 796.
3. Chandramouli, G. V. R.; Manoharan, P. T. *Inorg. Chem.* **1986**, *25*, 4680.
4. Isci, H.; Dağ, Ö.; Mason, W. R. *Inorg. Chem.* **1993**, *32*, 3909.
5. Goldoni, F.; Antolini, L.; Pourtois, G.; Schenning, A. P. H. J.; Janssen, R. A. J.; Lazzaroni, R.; Brédas, J.-L.; Meijer, E. W. *Eur. J. Inorg. Chem.* **2001**, 821.
6. Tastan, S.; Krause, J. A.; Connick, W. B. *Inorg. Chim. Acta* **2006**, *359*, 1889.
7. Grey, J. K.; Butler, I. S.; Reber, C. *Inorg. Chem.* **2003**, *42*, 6503.
8. Levasser-Thériault, G.; Reber, C.; Aronica, C.; Luneau, D. *Inorg. Chem.* **2006**, *45*, 2379.
9. Grey, J. K.; Butler, I. S.; Reber, C. *J. Am. Chem. Soc.* **2002**, *124*, 9384.
10. Yersin, H.; Donges, D.; Nagle, J. K.; Sitters, R.; Glasbeck, M. *Inorg. Chem.* **2000**, *39*, 770.
11. Ho, C.-L.; Wong, W.-Y. *J. Organometal. Chem.* **2006**, *691*, 395.
12. Akaiwa, M.; Kanbara, T.; Fukumoto, H.; Yamamoto, T. *J. Organometal. Chem.* **2005**, *690*, 4192.
13. Chakraborty, J.; Saha, M. K.; Banerjee, P. *Inorg. Chem. Comm.* **2007**, *10*, 671.
14. Kunkely, H.; Vogler, A. *Inorg. Chim. Acta* **2001**, *319*, 183.
15. Phadnis, P. P.; Jain, V. K.; Schurr, T.; Klein, A.; Lissner, F.; Schleid, T.; Kaim, W. *Inorg. Chim. Acta* **2005**, *358*, 2609.
16. Kang, J.-G.; Cho, H.-K.; Park, C.; Kang, S. K.; Kim, I. T.; Lee, S. W.; Lee, H. H.; Lee, Y. N.; Cho, S. H.; Lee, J. H.; Lee, S. H. *Bull. Korean Chem. Soc.* **2008**, *29*, 679.
17. (a) *SHELXTL*, 5.030 ed.; Brucker Analytical X-ray Instruments, Inc.: Madison, WI, 1998; (b) Sheldrick, G. M. *SHELEX97*; University of Göttingen, 1997.
18. Kang, J.-G.; Kim, T.-J.; Park, C.; Lee, S. W.; Kim, I. T. *Bull. Korean Chem. Soc.* **2004**, *25*, 704.
19. Yun, S.-S.; Kim, J.-K.; Jung, J.-S.; Park, C.; Kang, J.-G.; Smyth, D. R.; Tiekink, R. T. *Crystal Gowth & Design* **2006**, *6*, 899.
20. Noh, D.-Y.; Shin, K.-S.; Son, K.-I. *Bull. Korean Chem. Soc.* **2007**, *28*, 343.
21. *Gaussian 03*, Revision C.02; Gaussian, Inc.: Wallingford, CT, 2004.
22. Park, J. K.; Kim, B. G.; Koo, I. S. *Bull. Korean Chem. Soc.* **2005**, *26*, 1795.